

Shared Pump Two-Stage Polarization-Maintaining Holmium-Doped Fiber Amplifier

Robert E. Tench[✉], Senior Member, IEEE, Clement Romano[✉], and Jean-Marc Delavaux

Abstract—We propose and report the experimental demonstration of a shared pump architecture for a two-stage, broadband, high-gain polarization-maintaining Ho-doped fiber amplifier (H DFA). The gain as high as 59 dB, a noise figure of 10 dB, a dynamic range of >43 dB, and an output power of 4.1 W are achieved at a signal wavelength λ_s of 2051 nm. The multiwavelength performance of the H DFA is measured for $\lambda_s = 2004\text{--}2108$ nm. Initial comparisons of simulations with our experimental results show a relatively good agreement for $\lambda_s > 2051$ nm.

Index Terms—Doped fiber amplifiers, infrared fiber optics, optical fiber devices, holmium, polarization maintaining fiber, 2 microns.

I. INTRODUCTION

RECENTLY reported high gain Ho-doped fiber amplifiers are important for the development of high capacity WDM transmission systems and LIDAR applications in the 2000 nm band which require wide bandwidth, high gain, and large dynamic range optical amplifiers. Holmium-doped fiber amplifiers (HDFAs) are attractive for these applications because they extend the bandwidth response toward long wavelengths of 2000–2150 nm, a region not easily covered by Tm-doped fiber amplifiers. Also, HDFAs have high gain for wavelengths greater than 2050 nm, a region where Tm-doped fiber amplifiers exhibit low gain.

Several papers have presented results for amplifiers using single stage, single mode Ho-doped fibers. Filatova *et al.* [1] demonstrated $G > 35$ dB and $P_{out} = 1$ W with an amplifier pumped at 1125 nm, while Simakov *et al.* [2], [3] have reported $G = 40$ dB, $P_{out} = 0.25$ W, and noise figures $NF = 7\text{--}14$ dB. with HDFAs pumped at 1950–2008 nm. In addition, we have previously shown [4] high gain, two-stage PM HDFAs using two separate pumps with $G > 60$ dB, $P_{out} = 6.7$ W, a dynamic range of >40 dB, and $\eta = 80\%$.

While these results are encouraging, all the HDFAs so far reported employ one pump source for each optical amplifier stage, and results for PM HDFAs have been measured only

Manuscript received January 7, 2019; accepted January 23, 2019. Date of publication January 29, 2019; date of current version February 13, 2019. (*Corresponding author:* Robert E. Tench.)

R. E. Tench and J.-M. Delavaux are with Cybel LLC, Bethlehem, PA 18018 USA (e-mail: robert.tench@cybel-llc.com; jm@cybel-llc.com).

C. Romano was with Cybel LLC, Bethlehem, PA 18018 USA, and also with the Institut Telecom/Paris Telecom Tech, 75634 Paris, France. He is now with the Fraunhofer IOSB, 76275 Ettlingen, Germany (e-mail: clement.romano@iosb.fraunhofer.de).

Color versions of one or more of the figures in this letter are available online at <http://ieeexplore.ieee.org>.

Digital Object Identifier 10.1109/LPT.2019.2895786

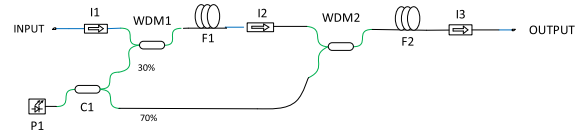


Fig. 1. Optical architecture for the shared pump PM H DFA.

for one signal wavelength ($\lambda_s = 2051$ nm). In this letter, we extend the measured performance of PM HDFAs by using a two-stage shared pump configuration and by investigating the performance of the amplifiers as a function of signal wavelength λ_s from 2004–2108 nm. We also extend our analysis by introducing simulated performance of the PM H DFA. Our studies show that the shared pump architecture is a simple, efficient, and high performance means of building two-stage PM HDFAs. This topology yields output power, gain, noise figure, and dynamic range results fully comparable with two-stage amplifiers constructed with two separate pump sources, and allows us to build versatile two-stage amplifiers.

II. EXPERIMENTAL SETUP

Figure 1 illustrates the optical architecture of the two-stage shared pump PM H DFA. A multiwatt PM fiber laser pump P1 at 1941 nm is divided by coupler C1 into a 30% output which pumps PM Ho-doped fiber F1 and a 70% output which pumps fiber F2. A 2004–2108 nm band single frequency input signal P_s (Eblana Photonics EP-2000 laser series) is amplified by F1, and the output of F1 is coupled into F2 for further amplification. F1 and F2 have lengths $L_1 = 3.0$ m and $L_2 = 2.0$ m, respectively.

In this setup, the first amplifying stage functions as a preamplifier, while the second stage is a power amplifier. Isolators I1–I3 in the signal path ensure unidirectional operation and suppress backward ASE. Signal and pump powers and noise figures are measured internally, and linearly polarized signal and pump light propagate through the amplifier along the slow fiber axis.

III. PM FIBER DATA AND APPROACH TO SIMULATIONS

Summary data for the iXblue PM Ho-doped single clad silica fiber in our experiments are given below in Table 1.

The fiber is designed for single mode operation in the 2000 nm band with a cutoff wavelength of 1650 nm.

Figure 2 shows gain and absorption spectra for the $^5I_7\text{--}^5I_8$ transition of the Ho-doped fiber, which were derived

TABLE I
PM HO-DOPED FIBER DATA

Fiber ID	IXF-HDF-PM-8-125
Core Diameter, μm	8
Cladding Diameter, μm	125
Numerical Aperture	0.15
Fiber Structure	PANDA
Birefringence	3.3×10^{-4}
Background Loss, dB/m	0.2
Peak Absorption, dB/m	57 @ 1951 nm
Ion Pairing Coefficient, %	10 (Ref. [5])
$^5\text{I}_7 - ^5\text{I}_8$ Radiative Lifetime, mS	9.67 (Ref. [6])
$^5\text{I}_7 - ^5\text{I}_8$ Nonradiative Lifetime, mS	0.60

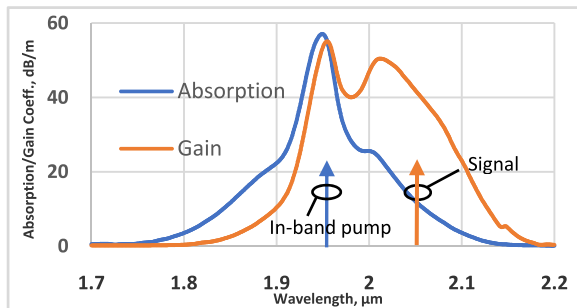


Fig. 2. Gain and absorption spectra for the Ho-doped fiber.

from measurements by iXblue and data from the literature [7]. The spectral region where the fiber exhibits significant gain clearly extends beyond 2150 nm.

Simulations of fiber performance used the gain and absorption spectra in Figure 1 and the data from Table 1 in a two-level Giles model [8] with a saturation parameter of $2.13 \times 10^{18} \text{ m}^{-1} \text{ s}^{-1}$ and internally developed code. The ion pairing coefficient accounts for loss of excited state ions caused by detrimental pairwise interactions [5]. In our experiments we chose in-band pumping with $\lambda_p \approx 1950 \text{ nm}$, close to the peak of the absorption as illustrated by the vertical blue arrow in Fig. 1.

The fiber lengths $L_1 = 3.0 \text{ m}$ (first stage) and $L_2 = 2.0 \text{ m}$ (second stage) were chosen by optimizing the first stage length for maximum simulated gain, and, subsequently, the second stage length for maximum simulated output power, for $\lambda_s = 2051 \text{ nm}$ and an available pump power of $P_p = 4.6 \text{ W}$ @ 1941 nm.

IV. EXPERIMENTAL AND SIMULATED RESULTS

Figure 3 plots the experimental gain G and noise figure NF (points) for the two-stage amplifier as a function of input signal power P_s , for a total 1941 nm pump power $P_p = 4.6 \text{ W}$ and $\lambda_s = 2051 \text{ nm}$. The maximum gain achieved is 59 dB, and the noise figure is 10 dB. For $G > 25 \text{ dB}$, the input signal dynamic

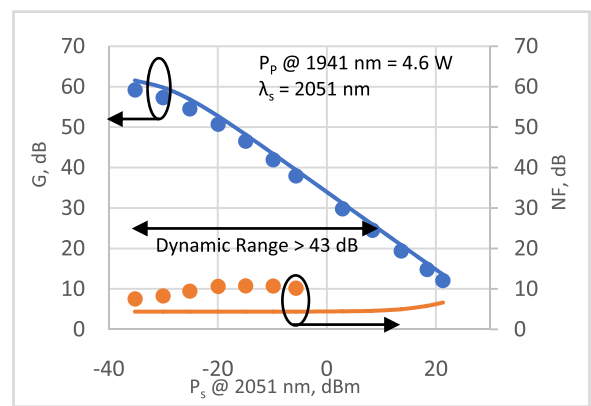


Fig. 3. G and NF vs. P_s for the two-stage amplifier: experiment and simulation.

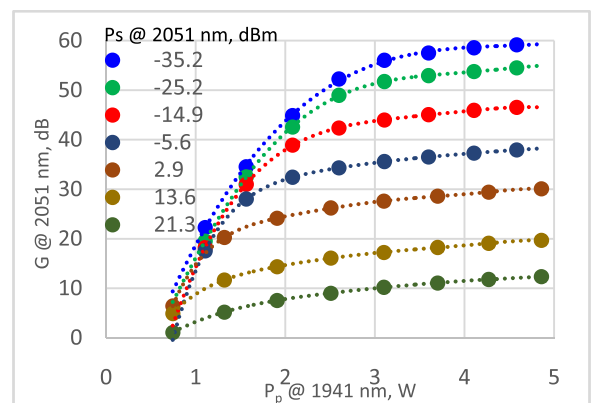


Fig. 4. G vs. P_p as a function of P_s .

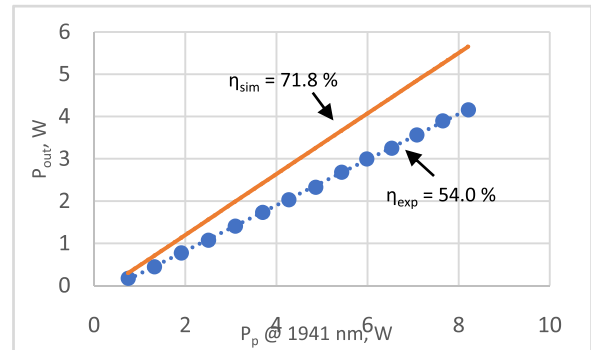


Fig. 5. Experimental and simulated P_{out} vs. P_p .

range of the amplifier is $> 43 \text{ dB}$. Simulations of G and NF , which are shown in solid lines, agree relatively well with the experimental data.

Figure 4 shows experimental G vs. P_p as a function of P_s , with P_s values ranging from -35 dBm to $+21 \text{ dBm}$. The dotted lines are polynomial fits to the data. For this amplifier, a pump power P_p of only 1.2 W is required to achieve a small signal gain of 25 dB , illustrating the efficient nature of the two-stage HDFA.

In Figure 5 we plot experimental (points) and simulated (solid line) values for output power P_{out} as a function of P_p ,

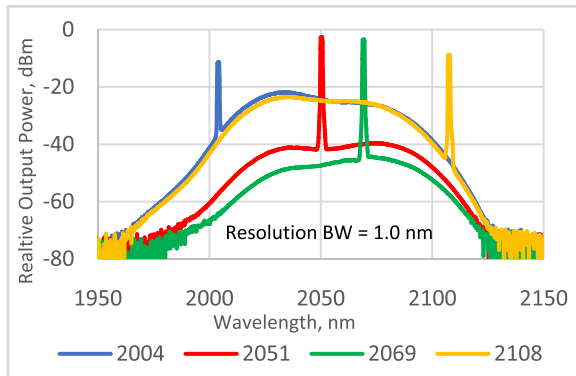


Fig. 6. Experimental output spectra for $P_s = -5$ dBm as a function of signal wavelength.

for $P_s = +21.3$ dBm at 2051 nm. Both the experimental and simulated P_{out} vary linearly with P_p , with optical-optical slope conversion efficiencies (defined as the change in P_{out} divided by the change in P_p or $\eta = \Delta P_{\text{out}}/\Delta P_p$), of $\eta_{\text{exp}} = 54.0\%$ and $\eta_{\text{sim}} = 71.8\%$. The difference between experimental and simulated output powers in this plot is 1.3 dB. A maximum output power of 4.15 W is achieved for $P_p = 8.2$ W. The difference between experiment and simulation may be caused by (1): Inaccuracies in the parameters used in the simulation, and (2): physical processes such as upconversion and SiOH impurity quenching which are not included in our two-level theory [9], [10].

Figure 6 illustrates output spectra for the two-stage amplifier as a function of λ_s from 2004–2108 nm, for $P_s = -5$ dBm and $P_p = 4.6$ W. We observe that P_{out} values for 2051 and 2069 nm are roughly equal, with diminished P_{out} at the outer limits of 2004 and 2108 nm. The optical saturation of the amplifier is strong for 2051 and 2069 nm as illustrated by the low ASE backgrounds for these two wavelengths. The optical saturation parameter is less for 2004 and 2108 nm, and this results in a higher ASE background. The operating bandwidth of the amplifier is seen to approach $BW = 80 - 100$ nm, consistent with the estimates given in [4].

Figure 6 shows that the measured optical signal to noise ratio (OSNR) of the signals varies from 52 dB/0.1 nm at 2069 nm to 37 dB/0.1 nm at 2004 nm. For single wavelength amplification a mid-stage ASE filter is expected to improve output power performance as demonstrated in [4].

In Figure 7 we plot experimental (points) and simulated (solid lines) G and NF as a function of λ_s for $P_s = -30$ dBm and $P_p = 4.6$ W. The dotted lines are polynomial fits to the data. Agreement between simulation and experiment for the gain is good for $\lambda_s \geq 2051$ nm. For $\lambda_s = 2004$ nm a significant deviation is apparent, with the observed gain 10–11 dB smaller, and the observed NF 16 dB larger, than the simulation. This difference, which is evident in the spectral plots of Figure 5, is currently under study. It may be caused by inaccuracies in the gain and absorption coefficients for the shorter wavelength region of the amplifier operating spectrum. It could also be caused by a signal wavelength close to the pump wavelength of 1941 nm, which may produce a lower effective experimental inversion in the fiber (compared to the simulated value).

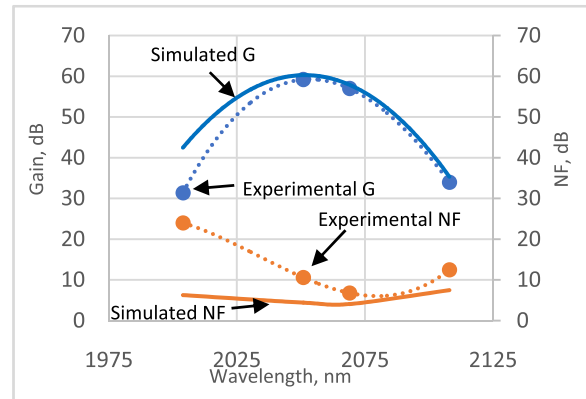


Fig. 7. Experimental and simulated G and NF vs. λ_s .

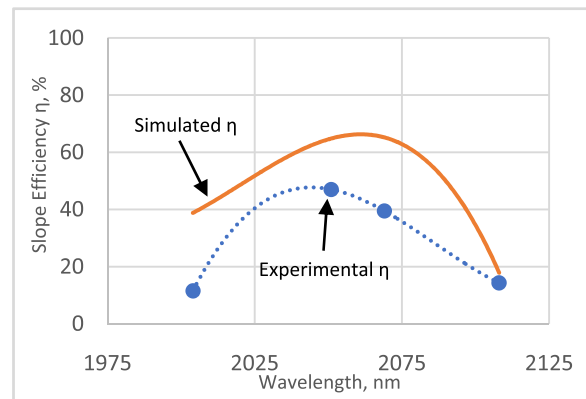


Fig. 8. Experimental and simulated η vs. λ_s for $P_s = -5$ dBm.

Figure 8 plots values of optical-optical slope conversion efficiency η for $P_s = -5$ dBm. In this figure, simulated values are given by the solid orange line, experimental data are plotted with blue points, and the dotted blue line is a polynomial fit to the data. For all wavelengths investigated, the simulation somewhat overpredicts the experimental slope efficiency. Nevertheless, the shape of the simulated curve generally follows the data.

V. DISCUSSION

The high gain of $G = 59$ dB, large dynamic range of >43 dB, and low noise figure of 10 dB for the two-stage shared pump PM HDFA are comparable to or better than the performance of a two-stage PM HDFA employing two separate pump sources [4]. Compared to this previous amplifier, the input signal dynamic range is increased by 3 dB and the noise figure is decreased by 4.5 dB. The decrease in noise figure is attributed to the low noise 1941 nm fiber laser pump source used in the shared pump amplifier, in contrast to a high amplified spontaneous emission noise MOPA pump source at 1952 nm that was employed in the first (preamplifier) stage of the PM HDFA with separate pump sources for two amplifier stages.

Experimental output powers as high as 4.2 W, and an experimental optical-optical slope efficiency $\eta = 54\%$, were achieved with the two-stage shared pump HDFA. We note that

this value is pump power limited, and we therefore expect to be able to scale to higher output powers by using more powerful fiber laser pump sources. No Brillouin scattering was observed up to the highest measured output power of 4.2 W. This observation is consistent with a preliminary calculation of $P_{out} = 50$ W for the onset of stimulated Brillouin scattering [11].

To estimate the potential effect of Raman gain on HDFA performance, we take $P_p = 8W$ @ 1941 nm, a fiber length of 5 m, and use the parameters from Table 1. We find [12] an upper bound on Raman gain at 2051 nm to be 0.3 dB. This estimate shows that Raman gain is not expected to contribute significantly to our experimental results.

The evolution of the output spectra for $\lambda_s = 2004\text{--}2108$ nm shows that the shared pump HDFA is capable of an operating optical bandwidth of $BW \approx 80\text{--}100$ nm. Future work will investigate the performance of the amplifier for wavelength outside of this region and also for additional signals in the range between 2020 nm and 2090 nm.

Simulated gains and noise figures agree relatively well with experiment for $\lambda_s \geq 2051$ nm. Future simulations will concentrate on the region near 2004 nm where a significant deviation between experiment and theory is observed, and study why the optical-optical slope efficiencies are overpredicted by the current theory.

VI. SUMMARY

We have reported the architecture, experimental performance, and simulated performance of a shared pump, two stage PM HDFA operating in the 2004–2108 nm spectral region. Our new amplifier design exhibits experimental results comparable to or better than a previous two stage PM HDFA employing separate pump sources for each amplifying stage. Comparison of experiment and simulation shows relatively good agreement, with some deviations between data and theory that are under active study. The new amplifier architecture results in a simpler, more efficient, and more compact two-stage PM HDFA for WDM lightwave systems and LIDAR systems, and represents a significant step forward in the design

of multi-stage optical amplifiers for applications operating in the 2000–2150 nm spectral region.

ACKNOWLEDGEMENTS

The authors thank iXblue for the PM Ho-doped fiber. They also thank Dr. Mahmood Bagheri of the Jet Propulsion Laboratory for the high power 2069 nm laser chip used as a signal source in the experiments, and Dr. Chris McIntosh of Army Research Labs for technical insight into Raman gain calculations.

REFERENCES

- [1] S. A. Filatova, V. A. Kamynin, V. B. Tsvetkov, O. I. Medvedkov, and A. S. Kurkov, "Gain spectrum of the Ho-doped fiber amplifier," *Laser Phys. Lett.*, vol. 12, no. 9, Aug. 2015, Art. no. 095105.
- [2] N. Simakov *et al.*, "High gain holmium-doped fibre amplifiers," *Opt. Express*, vol. 24, no. 13, pp. 13946–13956, Jun. 2016.
- [3] N. Simakov *et al.*, "Holmium-doped fiber amplifier for optical communications at 2.05–2.13 μm ," in *Proc. Opt. Fiber Commun. Conf. Exhib. (OFC)*, Mar. 2015, Paper Tu2C.6.
- [4] R. E. Tench, C. Romano, J.-M. Delavaux, T. Robin, B. Cadier, and A. Laurent, "Broadband high gain polarization-maintaining holmium-doped fiber amplifiers," in *Proc. Eur. Conf. Opt. Commun. (ECOC)*, Rome, Italy, Sep. 2018, Paper Mo3E.3.
- [5] A. S. Kurkov, E. M. Sholokhov, A. V. Marakulin, and L. A. Minashina, "Effect of active-ion concentration on holmium fibre laser efficiency," *Quantum Electron.*, vol. 40, no. 5, pp. 386–388, 2010.
- [6] R. Chen *et al.*, "Thermal and luminescent properties of 2- μm emission in thulium-sensitized holmium-doped silicate-germanate glass," *Photon. Res.*, vol. 4, no. 6, pp. 214–221, Dec. 2016.
- [7] N. Simakov, A. Hemming, W. A. Clarkson, J. Haub, and A. Carter, "A cladding-pumped, tunable holmium doped fiber laser," *Opt. Express*, vol. 21, no. 23, pp. 28415–28422, Nov. 2013.
- [8] C. R. Giles, C. A. Burrus, D. J. DiGiovanni, N. K. Dutta, and G. Raybon, "Characterization of erbium-doped fibers and application to modeling 980-nm and 1480-nm pumped amplifiers," *IEEE Photon. Technol. Lett.*, vol. 3, no. 4, pp. 363–365, Apr. 1991.
- [9] N. Simakov, "Development of components and fibres for the power scaling of pulsed holmium-doped fibre sources," Ph.D. dissertation, Univ. Southampton, Southampton, U.K., 2017.
- [10] J. Wang *et al.*, "Numerical modeling of in-band pumped ho-doped silica fiber lasers," *J. Lightw. Technol.*, vol. 36, no. 24, pp. 5863–5880, Dec. 15, 2018.
- [11] C. Romano, R. E. Tench, and J.-M. Delavaux, "5 W 1952 nm Brillouin-free efficient single clad TDFA," *Opt. Fiber Technol.*, vol. 46, pp. 186–191, Dec. 2018.
- [12] G. P. Agarwal, *Nonlinear Fiber Optics*. New York, NY, USA: Academic, 1995.